MSc in Photonics PHOTONICS**BCN**

Universitat Politècnica de Catalunya (UPC)
Universitat Autònoma de Barcelona (UAB)
Universitat de Barcelona (UB)
Institut de Ciències Fotòniques (ICFO)

http://www.photonicsbcn.eu

Master in Photonics

MASTER THESIS WORK

Conservation of Orbital Angular Momentum in Crystals with a Random Domain Distribution of Nonlinearity in SHG

Carlos Damián Rodríguez Fernández

Supervised by Dr. Jose Francisco Trull (UPC) and Dr. Alejandro Turpin (UAB)

Presented on date 7th September 2016

Registered at

Escola Tècnica Superior d'Enginyeria de Telecomunicació de Barcelona

Conservation of Orbital Angular Momentum in Crystals with a Random Domain Distribution of Nonlinearity

Carlos Damián Rodríguez Fernández

E-mail: carlos.damian.rodriguez@upc.edu.es

Abstract. In this master thesis we build an experimental setup for studying the conservation of the orbital angular momentum (OAM) of light in second harmonic generation (SHG) in Strontium Barium Niobate (SBN) crystals with random distribution of domains with inverted nonlinearity. Different methods to generate and measure OAM were implemented and the OAM conservation in SHG process in different kind of nonlinear crystals was studied. The experimental results point to the macroscopic non-conservation of the OAM in the family of nonlinear random crystals in SHG process.

Keywords: Orbital angular momentum, random nonlinear crystals, second harmonic generation.

1. Introduction

In 1992, Allen *et al*. demonstrated that light can carry orbital angular momentum (OAM) in addition to spin angular momentum (SAM). Moreover, they discovered an easy way to create beams carrying OAM in the laboratory by means of Laguerre-Gauss (LG) beams [1]. OAM is related to the phase structure of the light field. In particular, optical beams possessing an azimuthal phase dependence of the form $e^{il\varphi}$ carry a net amount l of OAM. This phase dependence manifests as a singularity at the beam centre and thus, at that point it possesses null intensity. For the case of LG beams, their shape depends on two indexes, p and l. The p index is the radial index indicating the number of radial nodes and is not related with OAM. The l index is the azimuthal index, and gives the value of the amount of OAM carried by the beam, $L = \pm l\,\hbar$ per photon. The simplest LG beams are the ones with $p = 0$, and an arbitrary azimuthal index l (doughnut shaped beams).

OAM is not only a curiosity but it is an interesting and useful property of light with powerful applications in recent research. For instance, it has served to trap and rote small particles thanks to the azimuthal gradient present in LG beams (optical spanners), to study the azimuthal Doppler Shift Effect -a technique allowing measuring the rotation speed of floating bodies, to create and manipulate quantum states in atomic ensembles able to storage information, or to increase channel capacity of information transmission systems [2, 3].

The OAM of light has also been a topic of study in the domain of NL (nonlinear) optics during the past years. Pioneering contributions demonstrated that OAM is conserved in second harmonic generation (SHG) processes in homogeneous NL crystals, analogously to energy conservation [4, 5]. In other words, for a given light beam at the fundamental frequency ω carrying $l\hbar$ OAM per photon, the SHG beam of frequency 2ω carries $2l\hbar$ per photon [4, 5]. More recently, OAM conservation was studied for different NL processes, symmetries and materials [7, 8]. However, OAM conservation in NL random crystals was not studied up to the present report. Previous related papers studied the OAM conservation in quasi-periodic $LiTaO_3$ poled crystals [8]. They

discovered that the quasi-periodic crystal splits the original beam in several SHG copies and that each copy conserves the OAM (it is doubled).

The motivation of this master thesis is to build an experimental setup to generate and measure OAM and use it to investigate OAM conservation in SHG processes occurring in crystals with a random distribution of domains with opposite quadratic nonlinear orientation which we call NL random crystals. The structure of this thesis is as follows: First, the OAM generation and measurement methods applied in the experimental setup are explained. Then, a brief description of the final experimental configuration is given. After that, the results are shown and discussed and finally, the conclusions are presented.

2. OAM generation

Generating beams with orbital angular momentum is the first step for studying OAM conservation in NL interactions. There are several ways to introduce OAM in beams: spatial light modulators (SLM), fork holographic gratings (FHG), q-plates, spiral plates, digital micro mirrors, mode-converters or conical refraction (CR) in biaxial crystals [2, 3]. In this master thesis, FHG, CR and SLM methods were studied. Each method has some advantages and some disadvantages, and they are used for different purposes in our experiment.

2.1 Fork Holographic Gratings

Fork holographic gratings (FHG) are holograms shaped with the interference pattern between a LG mode and a tilted plane wave. They have a fork-like structure which presents a singularity in the centre and a number of branches given by the OAM of the interfered LG mode [2, 3]. In figure 2a the interference pattern engraved in a FHG with l=2 is shown. Our FHG are designed to operate at 633 nm.

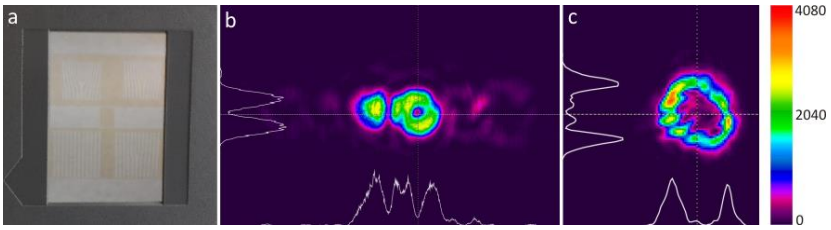

Figure 1 - a) Plate with different FHG designed for operate at 633 nm used in the laboratory b) Diffraction pattern of a FHG with l=1 at 633 nm. c) Filtered LG with l=5 generated by the correspondent FHG at 800 (note the worse quality).

When a plane wave passes through a FHG, its structure is changed. At the fourier plane of a lens a diffraction pattern with several discrete diffraction orders appears as depicted in figure 4c. The zero order is a gaussian beam without net OAM. The first orders are LG mode carrying the both senses of the OAM which was used to create the hologram. However, FHG are usually designed to produce only one intense first order to increase the generation efficiency as the experimental results of figure 1b shows. The rest of diffraction orders are very faint LG modes, with l increasing in one unit with the diffraction order.

The main drawback of FHG is that one needs one hologram for each mode and wavelength to be used. Moreover, it is necessary to filter the diffraction pattern to obtain a clean LG mode. Also replacing the hologram for generating other LG mode is slow because it requires aligning the

illumination and the filter in order to obtain good quality modes. The figure 1a shows the plate with the FHG used in the laboratory, 1b the LG generated with l=1 at 633 nm and 1c shows the LG mode for l=5 at 800 nm which has poor appearance due to the wavelength mismatch. The vertical and horizontal distributions in 1b and 1c are the vertical and horizontal intensity profiles of the beam integrated over the dotted lines of the plot. Regarding the colour scale, the warm tones represent high intensities and the cold ones low intensities in an arbitrary unit system. This format will be kept on the rest of figures of the present thesis.

2.2 Conical Refraction

Conical refraction is an optical phenomenon which allows to easily create intensity rings carrying and without carrying OAM exploiting the optical properties of birefringent crystals. The great advantage of this method is that one can work with intensity rings with and without OAM and compare the response of the studied crystals when the same light distribution carries OAM or not. As disadvantage, it is complex to operate with, and needs an accurate control of the polarization states of light. In the figure 3c one can see an intensity ring generated by conical refraction.

2.3 Spatial Light Modulators

Spatial Light Modulators are devices that introduce a controlled phase or intensity modulation in a light beam. They represent the most powerful way for light-shaping in conventional optical labs. Their screens contain liquid crystals whose orientation depend on the voltage applied and which control the phase and intensity changes of the beam at each point of the screen. The SLM we used is a Hamamatsu PPM X8267-16 designed for operating from 400 to 700 nm. The phase structure to insert in the beam is sent to the SLM though an image where the grey level value of each pixel codifies the phase modulation at each point of the SLM screen.

There are several ways to create beams with OAM using a SLM. One of them is displaying on the SLM the pattern of the FHG used in the previous section. The pattern is rapidly generated simulating the corresponding interference and it can be tuned changing the position of the central node and the angle between the interfering waves. The output is a diffraction pattern similar to the FHG case. The principal con is that the energy of the input beam is strongly distributed over the different diffraction orders so there is not enough energy for SHG. Figure 2 shows some digital diffraction patterns and the corresponding diffraction modes for a He-Ne laser operating at 633 nm.

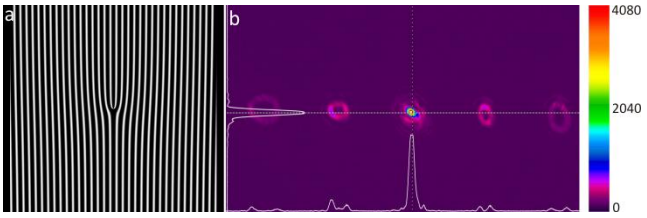

Figure 2 – a) Digital FHG for l=2. b) Its diffraction pattern containing different LG modes. The order zero has l=0, the first orders of diffraction are l=2, the second ones are l=3, etc Notice the increment of the ring radius with l.

Other option to create an optical vortex is to directly insert in the input beam a spiral phase structure $e^{il\varphi}$. This approach has the advantage that the beam is not splitted in diffraction orders so, at the output, there is only a LG beam with energy enough for produce SHG. Figure 3a shows a $l = 4$ spiral phase structure, and 3b the corresponding LG mode.

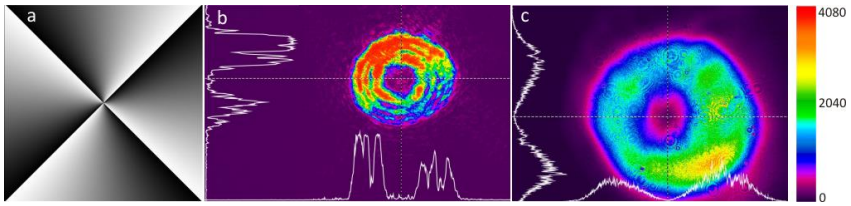

Figure 3 – a) Spiral phase structure for l=4. b) LG mode generated with laser at 633 nm. c) Ringed intensity profile generated by conical refraction without net OAM.

3. OAM Measurement

There are several ways to measure the OAM carried by a beam. Some techniques are interference, mode converters, tilted lenses, cylindrical lenses or holograms. In this master thesis, the methods experimentally studied for detecting OAM are interferometry, mode-converters and cylindrical lenses.

3.1 Interferometry

The interference pattern of a LG beam with a reference wave depends on the reference wave and on the angular momentum carried by the LG beam. First, the input beam is divided in two before the LG mode generator. The LG mode is generated in one of the two paths. After that, both paths recombine and the interference pattern appears. When the reference wave is a spherical wave, the interference pattern forms a spiral whose number of branches is given by the OAM of the beam. When the reference wave is a tilted plane wave, the mentioned fork interference patterns appear. The number of dislocations in these fork-patterns is the same as the OAM carried by the LG beam [2, 3]. The main problem with interferometry is that the beam carrying OAM only possesses half the laser energy due to the beam splitting. Additionally, to use this technique with SHG processes, the frequency of the reference beam must be doubled by two as well. Moreover, if the coherent length of the laser is not too large, interference will not happen. In figure, 4 fork interference patterns obtained with a He-Ne laser operating at 633 nm are shown.

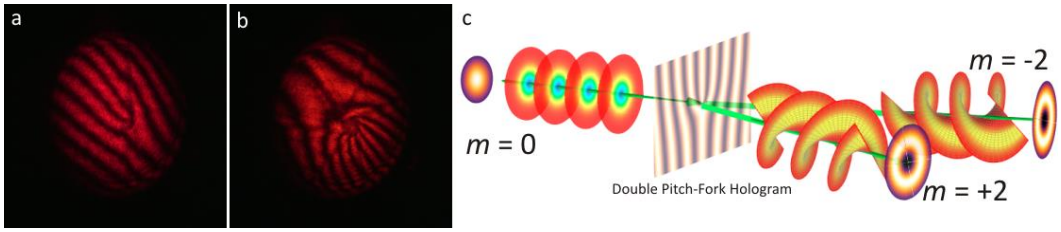

Figure 4 - a) Fork interference pattern for l=2. b) Fork interference pattern for l=-7.c) Plane wave passing through a FHG with l=2. Only the first orders corresponding with l=±2 are shown. Wikimedia commons. Author: E-karimi

3.2 Mode-converter

Mode converters are optical devices which decompound the basis of an input beam into modes of other basis in the output beam. That is, the mode expansion in which the beam was expressed is changed [3]. There are several types of mode converters; we will focus on π/2 converters which transform HG modes into LG modes and vice versa. They consist on two cylindrical lenses with the same focal length, f, which are separated a distance given by $\sqrt{2}\,f$. The focal length of the cylindrical lens is chosen according to the size of the beam when it is focused on the middle of both lenses [2]. LG modes with $p = 0$ and a certain l, are converted into only one HG mode with

$m = 0$ and $n = l$. These modes have the same number of nodal fringes as its n value. Thus, the number of fringes of the converted beam directly allows one to measure the amount of OAM carried by the original beam. Since mode converters are complex to work with, when no exact transformation of modes is required, cylindrical lens method is an easier option to implement. Figure 5 contains some conversions of LG modes into HG modes using a π/2 mode converter. In 5a and 5c, LG modes with l=±3 are shown. These modes are converted into HG modes with three dark fringes in 5b and 5d. The orientation of the fringes is different in both cases due to the difference in the sense of the OAM of the original LG modes.

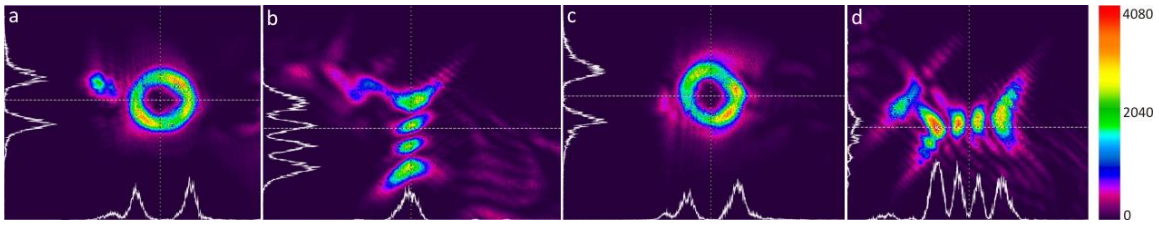

Figure 5 - a) LG mode with l=3 with contribution of the l=0 mode. b) HG conversion of the LG l=3. c) LG with l=-3. d) HG conversion of LG with l=-3. Note the change in the orientation in the HG modes.

3.3 Cylindrical lens method

The cylindrical lens method is a simplification of the mode converter method. Here, the astigmatism of the cylindrical lens is used to deform the optical vortex in such a way that a set of dark fringes appear in the output beam. The number of dark fringes is the same as the OAM carried by the LG beam [8]. It was the chosen method for implement in the final experimental setup. Figure 6 shows OAM measurement of a LG beam with $l = 20$ using the cylindrical lens method.

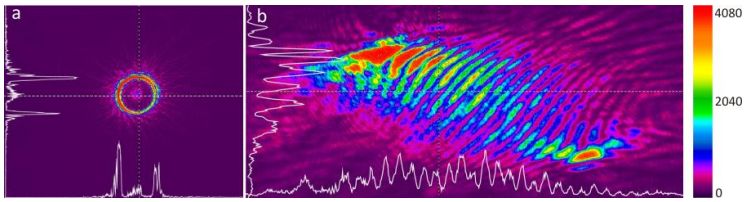

Figure 6- a) LG mode with l=20. Cylindrical lens transformation with 20 dark fringes.

4. Experimental setup

The main purpose of the present master thesis is to build an experimental setup to generate and measure angular momentum and to measure the SHG signal of a LG beam in a random NL crystal. The experimental setup evolved continuously up to reach the final form of the figure 7.

The two laser sources, He-Ne (align) or Ti:Saphire (SHG) after being expanded by a factor of 2, in order to cover the spatial size of the SLM, can be introduced at will in the angular momentum generation part. Since we used different methods, a flip mirror was used to switch between the FHG/CR or the SLM mode. In the FHG mode, the diffraction pattern containing the different LG modes generated appears in the fourier plane of a microscope objective. This diffraction pattern is then filtered to choose the desired LG mode. Another microscope objective recovers the beam original size and then the LG mode is focused with a lens into the NL crystal. In the case of OAM generation by CR, a quarter wave plate is used to obtain circular polarization and then it is

focused inside a birefringent KTP crystal. The intensity rings generated have opposite circular polarizations and can be individually selected using a circular polarization selector. After, the intensity ring is focused in the NL crystal. In the SLM case, the beams are expanded conveniently in order to cover the spatial size of the SLM screen and then it is reflected with the phase structure desired. The LG mode appears in the fourier plane of a lens which directly focalizes in the NL crystal. The SH intensity is optimized using a half wave plate. For the case of the random NL crystal, the SH is emitted over a line as explained later. In order to study the SH emission over the line we mounted a mobile OAM measuring branch. For the measurement part, each branch (fixed and mobile) has an imaging system composed by a lens which images the beams in a CCD camera and also an optional OAM-meter based on the cylindrical lens method explained previously.

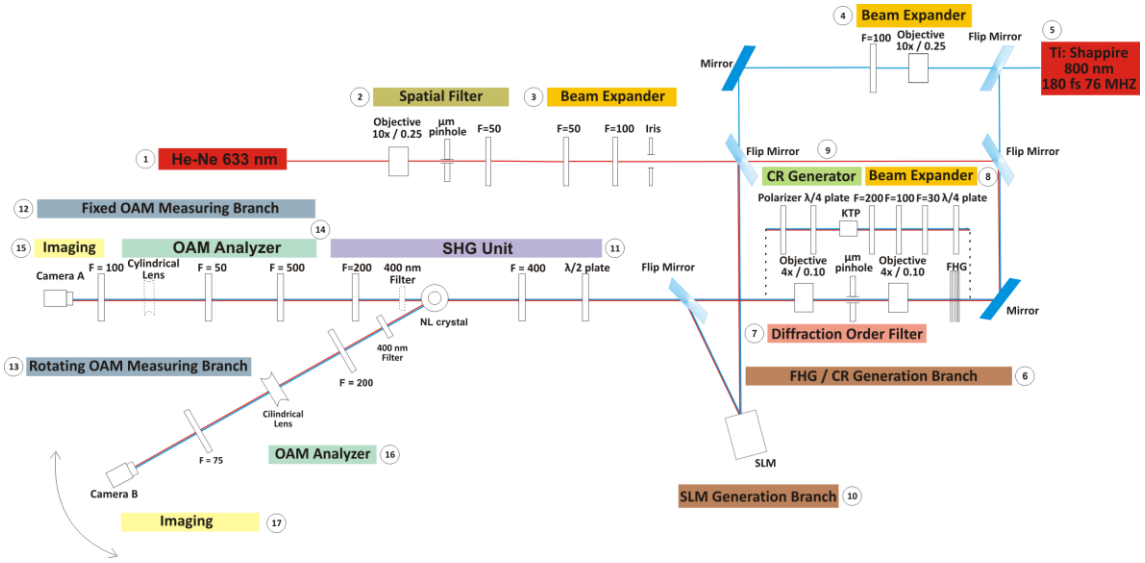

Figure 7 - Scheme of the experimental setup.

5. Results & Discussion

OAM conservation in SHG processes was studied inside a standard birefringent BBO crystal and in Strontium Barium Niobate (SBN) crystals which possess a random-size distribution of domains with inverted direction of their quadratic nonlinearity which generically are called NL random crystals. In the BBO crystal, when the polarization and direction of propagation of the incoming light are correctly set, phase matching condition is satisfied and SHG occurs. In this process, two photons of the input beam (Ti:Saphire, 800 nm) are converted in one photon of the output beam (400 nm) doubling frequency and OAM [4]. This fact is consistent with our results, which show the OAM doubling in the SHG process, as shown in figure 8. There, 8a shows a LG beam with l=3 and 8b the correspondient cylindrical lens decomposition with three dark fringes. The doubled LG is shown in 8c where the ring is a bit deformed and the corresponding cylindrical lens decomposition is 8d which shows six dark stripes which proof the OAM conservation in the SHG process.

Our NL random crystals are made of domains of random size with inverted direction of their quadratic nonlinearity distributed around a certain mean value which is different for each crystal.

In our samples, this mean size varies from nanometres to microns. The domains are spatially oriented along the optical axis. The random size of the domains offers an infinite set of reciprocal lattice vectors, $\boldsymbol{G}$ which allow phase matching in the plane perpendicular to the optical axis As a consequence, the SH signal of random crystals is radiated over a plane creating an emission line instead of a punctual emission [9]. Figure 9 shows a representation of the domains of one of the studied crystals as well as a scheme of the phase matching condition.

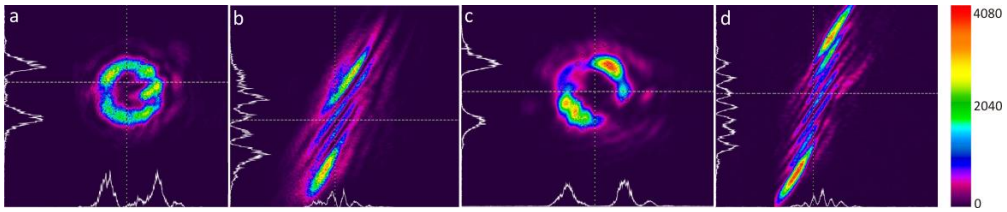

Figure 8 - a) LG with l=3. b) Cylindrical lens method for l=3. c) SHG of the beam in a) with doubled OAM l=6. d) Cylindrical lens transformation of the beam in c), possessing 6 dark fringes.

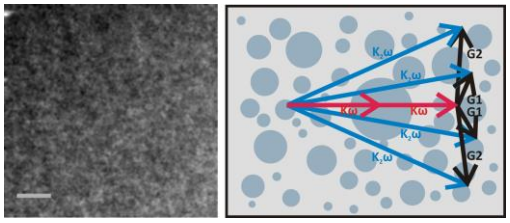

Figure 9 - a) Transversal image of the random domain in a random crystal. b) Random phase matching.

Three different kinds of beams were sent to the NL random crystals: gaussian beams without OAM, ring-shaped LG beams with a net OAM and ring-shaped beams without OAM. All of them were sent into the random crystals in a direction perpendicular to the optical axis. The experimental results described below were observed in all the random crystals studied without obtaining any important qualitative difference between them despite the differences in the mean size of its domains. The emission of the crystals was measured from different directions using the rotating and fixed branches of the experimental setup. In the fixed branch, which coincides with the direction of propagation of the fundamental beam, two transverse imaging planes were of interest: the plane where SHG process is initiated inside the crystal which we call generation plane and one of the planes where the net effect of the SHG process along the crystal is observed which we call net effect plane. In the angular branch, the generation plane is tilted respect to the camera; thus in this branch, only the angular net effect plane is imaged which we simply call angular plane.

When a gaussian beam with l=0 is sent to the NL random crystal, it radiates a single emission line, as was expected according to [9]. The emission line is confined in a plane perpendicular to the growth direction of the ferroelectric domains. This plane contains the $\boldsymbol{G}$ vectors of the lattice formed by the random ferroelectric domains, which lead to a SHG phase matching situation similar to the quasi-phase matching one where the discrete distribution of $\boldsymbol{G}$ is now continuous. As a consequence, rotating the crystal around its optic axis rotates the plane of the emission line. In the angular plane and the SHG net effect plane only this single line is imaged as one can see in the figure 10b. However, in the generation plane, the gaussian distribution of the fundamental beam is seen in the doubled signal as is depicted in the zero diffraction order of figure 10a.

For ring-shaped LG beams carrying an OAM $l \neq 0$, the random crystal emission was observed to be similar independently of the l carried by the beam. In this case, the emission consists in two very close parallel lines which can be seen in figures 11c and 11d. In the generation plane, the LG mode of the fundamental beam is observed in the second harmonic signal as one can see in the first diffraction order of the figure 11a. However, this second harmonic intensity ring is not homogenous as the fundamental signal ring was; it is significantly more intense in some parts than in others. This means that the SH conversion efficiency is not homogenous along the fundamental ringed intensity. When the crystal is rotated about its optic axis, the SH efficiency along the fundamental beam changes in such a way that the most intense parts of the second harmonic rings are not the same as before. This SHG efficiency change goes with a rotation of the emission plane as occurred above. In the angular plane and the net effect plane what is observed are the two parallel lines previously mentioned of the figures 11c and 11d. In the planes between the generation plane and the net effect plane, it is possible to see how the SH ring breaks and evolves to become into the two parallel lines.

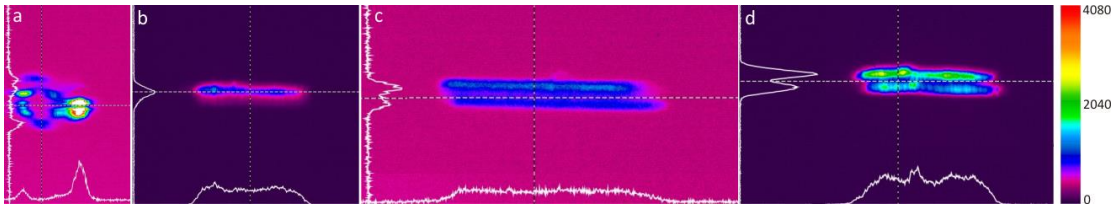

Figure 10 - a) SHG of the zero (l=0) and first diffraction order (l=5) on the SHG plane of a random crystal. b) SHG emission of the random crystal for the zero order, l=0. c) SHG emission for the first order, l=5. d) SHG emission for other beam with l=1. No substantial differences are found between l=1 and l=5 SHG emissions.

The changes in the SHG efficiency along the fundamental doughnut distribution are related with changes in the phase matching condition along the intensity distribution of the fundamental signal. As commented above, the reciprocal $\boldsymbol{G}$ vectors of the crystal are confined in a plane perpendicular to the growth direction of the domains. The propagation $\boldsymbol{k}$ vectors of the fundamental beam are different along the doughnut. When the $\boldsymbol{k}$ vectors are closely parallel to the plane containing the $\boldsymbol{G}$ vectors, there is a large amount of reciprocal vectors able to fulfil the phase matching condition. In contrast, $\boldsymbol{k}$ vectors of the fundamental beam laying in different planes to the plane of the $\boldsymbol{G}$ vectors, do not contribute to SHG. Thus, the parts of the LG mode which perfectly fulfil the phase matching condition become frequency doubled while this process is very inefficient in parts which weakly satisfy the phase matching condition. When the crystal is rotated, the position of the plane of the reciprocal $\boldsymbol{G}$ vectors change respect to the incoming beam so the parts which before were under phase mismatch now are under phase matching and vice-versa. It coincides with the experimental observations in which the parts of the LG mode efficiently converted changed rotating the random crystal about its optic axis. This non-homogenous efficiency of the SHG along the fundamental intensity distribution points to a possible degradation of OAM in the process.

Finally, for ring-shaped beams without OAM, which were generated by means of the conical refraction method, the observed experimental behaviour of the SH signal generated was the same as the case of ring-shaped beams with net OAM. No remarkable differences were found between rings with and without OAM. In a recent article [8], OAM conservation in SHG process inside a periodically poled $LiTaO_3$ crystal was studied. $LiTaO_3$ crystals are periodical structures which

facilitate phase matching through the quasi phase matching method. In this family of crystals, there is only a reciprocal vector $\boldsymbol{G}$, so the compensation of the phase mismatch is carried out through $\boldsymbol{G}$ or integer multiples of $\boldsymbol{G}$. In [8], the authors observed that when a LG beam is introduced in the $LiTaO_3$ crystal, multiple copies of LG beams with doubled OAM are obtained. These multiples copies arise due to the integer multiples of $\boldsymbol{G}$ make possible satisfy the phase matching condition simultaneously in collinear and non-collinear geometry. The SH copies obtained of the fundamental beam were clearly separated in the same emission line according to the geometry which produced them. In our NL random crystal case the situation is similar but different. In this case, there is not only one $\boldsymbol{G}$ and its multiples, but there is a continuous set of reciprocal $\boldsymbol{G}$ vectors allowing continuous phase matching for all the $\boldsymbol{k}$ vectors of the input beam lying in the same plane than $\boldsymbol{G}$ vectors. That is the reason why, we do not expect to obtain isolated doubled LG modes in the emission line but an emission line made of continuously superposed doubled LG modes. In order to study how the obtained experimental results could match this hypothesis, we have carried out different numerical simulations were LG beams of the same order were added in a line with different separation distances between rings and in two different fashions: coherently and incoherently as one can see in figure 11a and 11b respectively.

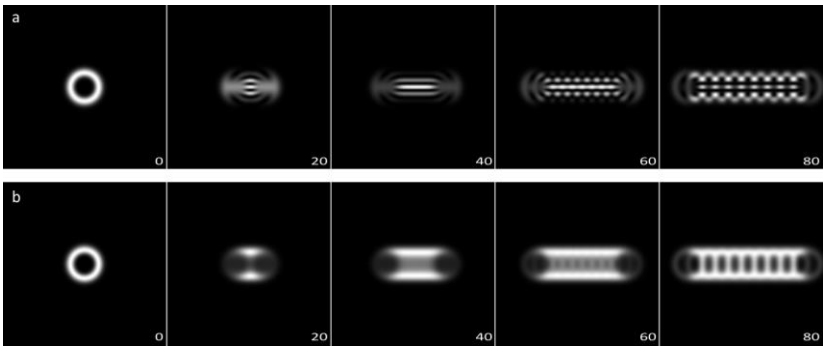

Figure 11 - Sum of LG modes with l=6 and ω_0=50 au for different separation distances in au (right inferior corner of each image). a) Coherent sum b) Incoherent sum

In the coherent sequence of figure 11a, the simulations show complex interference patterns which depend on the l of the generated LG mode. These complex patterns were not observed experimentally for any l. In fact, no significative differences were observed between different input OAM values. In the incoherent sequence of figure 11b, the intensity pattern obtained is not strongly dependent on the OAM carried by the input beam and the different rings of the different LG modes only can be seen when the separation distance between modes is large enough. These incoherent simulations remind two intense parallel lines with a region of lower intensity between them. These incoherent patterns agree with the experimental emission line obtained in the laboratory for the NL random crystals studied. As the SH emission line of the NL random crystal studied agrees with an incoherent addition of LG modes of the same order very near ones from other, the line obtained is expected to lack of net OAM due to the intrinsic incoherence of the addition between rings, that is, even if each single ring holds its OAM and it is doubled, when it is superposed with another ring on a incoherently way, the result has not a well-defined OAM. The introduction of cylindrical lenses in the detection path did not reveal new information about the OAM conservation in the output beam, i.e., the transformation did not present any clear dark fringe. These results agree with the incoherent nature of the SH emission line of the NL random

crystal noted in previous works [10]. These results point to the macroscopic OAM degradation of the output beam while at the photon level, OAM is expected to be conserved considering the interaction with the random crystal. This degradation occurs due to the inhomogeneous SHG efficiency along the LG mode but also to the incoherent superposition in the output of a large number of LG beams.

Conclusion

In this master thesis, an experimental setup was built to study several ways to create and measure OAM. The obtained techniques were used to study the OAM conservation in SHG in standard NL crystals and NL random crystals. In random crystals, macroscopic non-conservation of OAM was observed. There are two main factors which explain the degradation of the OAM in the SHG process: first, the efficiency of generation is not homogenous along the fundamental LG intensity distribution due to its distribution of $\boldsymbol{k}$ vectors; and second, the continuous set of $\boldsymbol{G}$ vectors provided by the random crystal produce an emission line composed by an incoherent continuous distribution of LG modes arbitrarily near ones from others. Up to now, this is the first time which the macroscopic OAM conservation is violated in a SHG process. However, the experiment can be improved in order to obtain clearer and more conclusive results. For instance, it is possible to study OAM conservation in SHG process when light arrives to the NL random crystal parallel to its optical axis or introduce an OAM-meter based on interferometry to study the SH signal more in deep. Another way to obtain clearer results is improve the technical features about the experiment, for example, using a SLM operating at 800 nm to observe in real time and in the same conditions the changes in the emission when different OAM is sent to the crystals. Due to all these motives and because improvement is possible, we will keep working hard in this research line trying to obtain our best efforts and the best reachable results.

6. Bibliography

[1] L. Allen, M.W. Beijersbergen, R.J.C. Spreeuw, and J.P. Woerdman 1992 Orbital angular momentum of light and the transformation of Laguerre-Gaussian laser modes Physical Review A Volume **45**, number 11.

[2] Yao, A.M., and Padgett, M.J 2011 Orbital angular momentum: origins, behavior and applications Advances in Optics and Photonics, **3**.

[3] J. Arlt, K. Dholakia, L. Allen, and M. J. Padgett 2004 Light's Orbital Angular Momentum Physics Today

[4] K. Dholakia, N. B. Simpson, and M. J. Padgett and L. Allen, 1996 Second-harmonic generation and the orbital angular momentum of light Physical Review A Volume **54**, number 5.

[5] J. Courtial, K. Dholakia, L. Allen, and M. J. Padgett 1997 Second-harmonic generation and the conservation of orbital angular momentum with high-order Laguerre-Gaussian modes Physical Review A Volume **56**, number 5.

[6] J. Arlt, K. Dholakia, L. Allen, and M. J. Padgett 1999 Parametric Down-conversion for light beams possessing orbital angular momentum Physical Review A Volume **59**, number 5.

[7] Thomas Roger, Julius J. F. Heitz, Ewan M. Wright & Daniele Faccio 2013 Non-collinear interaction of photons with orbital angular momentum Scientific Reports **3**:3491.

[8] Xinyuan Fang, Dunzhao Wei, Dongmei Liu, Weihao Zhong, Rui Ni, Zhenhua Chen, Xiaopeng Hu, Yong Zhang and S. N. Zhu 2015 Multiple copies of orbital angular momentum states through second-harmonic generation in a two-dimensional periodically poled LiTaO3 crystal Applied Physics Letters 107, 161102 (2015); doi: 10.1063/1.4934488.

[9] R. Fischer, S. M. Saltiel, D. N. Neshev, W. Krolikowski, and Yu. S. Kivshar 2006 Broadband femtosecond frequency doubling in random media Applied Physics Letters 89, 191105 (2006); doi: 10.1063/1.2374678.

[10] J. Trull, C. Cojocaru, R. Fischer, S.M. Saltiel, K. Staliunas, R.Herrero, R.Vilaseca, D. N. Neshev, W. Krolikowski and Y.S. Kivshar 2007 Second-harmonic parametric scattering in ferroelectric crystals with disordered nonlinear domain structures Optics Express Vol. **15**, No. 24 / 15877